NBI-HE-00-24
NORDITA-2000/50-HE
hep-th/0005147
May 2000

Monte Carlo Studies of the IIB Matrix Model at Large N

J. Ambjørn[1)*], K.N. Anagnostopoulos[2)†],
W. Bietenholz[3)‡], T. Hotta[4)§] and J. Nishimura[1)¶]

[1)] *Niels Bohr Institute, Copenhagen University,*
Blegdamsvej 17, DK-2100 Copenhagen Ø, Denmark
[2)] *Department of Physics, University of Crete,*
P.O. Box 2208, GR-71003 Heraklion, Greece
[3)] *NORDITA*
Blegdamsvej 17, DK-2100 Copenhagen Ø, Denmark
[4)] *Institute of Physics, University of Tokyo,*
Komaba, Meguro-ku, Tokyo 153-8902, Japan

Abstract

The low-energy effective theory of the IIB matrix model developed by H. Aoki et al. is written down explicitly in terms of bosonic variables only. The effective theory is then studied by Monte Carlo simulations in order to investigate the possibility of a spontaneous breakdown of Lorentz invariance. The imaginary part of the effective action, which causes the so-called sign problem in the simulation, is dropped by hand. The extent of the eigenvalue distribution of the bosonic matrices shows a power-law large N behavior, consistent with a simple branched-polymer prediction. We observe, however, that the eigenvalue distribution becomes more and more isotropic in the ten-dimensional space-time as we increase N. This suggests that if the spontaneous breakdown of Lorentz invariance really occurs in the IIB matrix model, a crucial rôle must be played by the imaginary part of the effective action.

*e-mail address : ambjorn@nbi.dk
†e-mail address : konstant@kiritsis.physics.uoc.gr
‡e-mail address : bietenho@nordita.dk
§e-mail address : hotta@hep1.c.u-tokyo.ac.jp
¶Permanent address : Department of Physics, Nagoya University, Nagoya 464-8602, Japan,
e-mail address : nisimura@nbi.dk

1 Introduction

For more than two decades superstring theories have been studied as the most promising candidates for a unified theory of all the interactions including gravity. The theories have the potential to predict the space-time dimensionality, the gauge group, the matter content, and so on, from first principles. The existence of infinitely many perturbative vacua implies, however, that an understanding of nonperturbative effects is crucial to extract information about the real vacuum of the theory. Recent proposals for nonperturbative formulations of superstring theories [1, 2, 3, 4, 5] may therefore be of analogous importance for our understanding of non-perturbative aspects of string theory as lattice gauge theory [6] has been in understanding nonperturbative dynamics of gauge theories. The IIB matrix model [2], which is conjectured to be a nonperturbative formulation of type IIB superstring theory (for a review, see Ref. [7]), takes the form of a large N reduced model [8], and in the same way that Monte Carlo studies of lattice gauge theory clarified many important nonperturbative aspects of the strong interaction, Monte Carlo studies of the IIB matrix model might illuminate the nonperturbative dynamics of superstring theories[1]. A number of numerical studies have already been done [10, 11, 12, 13, 14, 15, 16, 17, 18, 19] to pursue that direction. Earlier numerical studies of *world-sheet perturbative* aspects of superstring-like theories can be found in Refs. [20, 21, 22].

In this paper, we study the IIB matrix model at large N by Monte Carlo simulations. In particular, we investigate the possibility of a spontaneous symmetry breakdown of Lorentz invariance using the low-energy effective theory of the IIB matrix model proposed by Ref. [23]. The authors of [23] also study this issue, using an approach where the bosonic and fermionic matrices are both decomposed into diagonal elements and off-diagonal elements, and the off-diagonal elements are integrated out first perturbatively. Such a perturbative expansion is valid when the bosonic diagonal elements, which can be regarded as coordinates of N points in ten-dimensional flat space-time, are well separated from each other. In other words, what one obtains after integrating over the off-diagonal elements perturbatively can be considered as a low-energy effective theory of the IIB matrix model. Note that this perturbative expansion has nothing to do with the string perturbative expansion with respect to the world-sheet topology. Therefore, even at the one-loop level, the low-energy effective theory is expected to include *nonperturbative* effects of superstring theory, provided, of course, that the IIB

[1] Monte Carlo studies of Matrix Theory [1] would be technically more involved due to a lattice discretization of the time direction [9].

matrix model conjecture is true.

In fact, in order to obtain the low-energy effective action only for the bosonic diagonal elements, one still has to perform the integration over the fermionic diagonal elements, which is nontrivial, since their action turns out to be quartic. Although the explicit form of the final low-energy effective theory has not been derived, the theory was shown [23] to be described by some complicated branched-polymer like system, typically involving a "double-tree" structure, in a flat ten-dimensional space time. Thus, even at the one-loop level[2], the low-energy effective theory contains highly nontrivial dynamics. It was further argued that the double-tree structure of the one-loop low-energy effective theory might be responsible for a collapse of the distribution of the bosonic diagonal elements. The first Monte Carlo results of a branched-polymer system with a double-tree structure was reported in Ref. [7].

Here, we write down explicitly the low-energy effective theory of the IIB matrix model in terms of bosonic variables only. Instead of integrating over both bosonic and fermionic off-diagonal elements first, we leave the bosonic off-diagonal elements unintegrated. The action for the fermionic diagonal elements is then still quadratic and can be integrated explicitly, yielding a Pfaffian. Integration over the bosonic off-diagonal elements as well as the bosonic diagonal elements can be done by Monte Carlo simulation. In other words, the bosonic off-diagonal elements play the rôle of auxiliary variables, which enable us to simulate the complicated branched-polymer like system describing the dynamics of the bosonic diagonal elements.

The Pfaffian induced by the integration over the fermionic diagonal elements is generically complex. In general, when the action of a theory has a non-zero imaginary part, the number of configurations needed to extract any information increases exponentially with the system size, except in a few situations, where alternative sampling methods can be invented [24, 25]. This notorious technical problem in Monte Carlo simulations is known as the "sign problem". In fact, the problem exists already in Monte Carlo simulations of the original IIB matrix model and it is inherited by the low-energy effective theory. In the present work, we simply use the absolute value of the Pfaffian in order to avoid the sign problem and examine only the effect of the modulus of the Pfaffian. Our results suggest that there is no spontaneous symmetry breakdown (SSB) of Lorentz invariance. From this we conclude that if the SSB ever occurs in the IIB matrix model, the phase of the Pfaffian must play a crucial rôle.

[2]The validity of the one-loop approximation for studying the low-energy dynamics of supersymmetric large N reduced models has been demonstrated in Ref. [18] through the study of the four-dimensional version of the IIB matrix model. We will come back to this point is Section 3.

We also study the six-dimensional version of the IIB matrix model for comparison. The conclusion is the same, but we find an intriguing difference in the finite N effects.

The paper is organized as follows. In Section 2, we describe the definition of the IIB matrix model and review some important properties relevant for this work. In Section 3, we derive the low-energy effective theory of the IIB matrix model and explain the model we investigate by Monte Carlo simulations. In Section 4, we present our results for the distribution of the bosonic diagonal elements. In particular, we discuss the possibility of SSB of Lorentz invariance. Section 5 is devoted to a summary and conclusions. In Appendix A, we explain the details of the algorithm we use for the Monte Carlo simulation. In Appendix B, we present some systematic studies for optimizing the parameters involved in the algorithm.

2 The IIB matrix model

The IIB matrix model [2] is formally a zero-volume limit of ten-dimensional pure $\mathcal{N} = 1$ supersymmetric Yang-Mills theory. The action, therefore, is given by

$$Z_{\rm IIB} = \int \mathrm{d}A \; \mathrm{e}^{-S_{\rm b}} Z_{\rm f}[A] \quad ; \quad Z_{\rm f}[A] = \int \mathrm{d}\psi \; \mathrm{e}^{-S_{\rm f}} \; , \tag{2.1}$$

$$S_{\rm b} = -\frac{1}{4g^2} \mathrm{tr}([A_\mu, A_\nu]^2) \; , \tag{2.2}$$

$$S_{\rm f} = -\frac{1}{2g^2} \, \mathrm{tr} \left(\psi_\alpha (\tilde{\Gamma}_\mu)_{\alpha\beta} [A_\mu, \psi_\beta] \right) \; . \tag{2.3}$$

A_μ ($\mu = 1, \cdots, 10$) and ψ_α ($\alpha = 1, \cdots, 16$) are $N \times N$ traceless Hermitian matrices, which can be expanded in terms of the generators t^a of SU(N) as

$$(A_\mu)_{ij} = \sum_{a=1}^{N^2-1} A_\mu^a \, (t^a)_{ij} \qquad ; \qquad (\psi_\alpha)_{ij} = \sum_{a=1}^{N^2-1} \psi_\alpha^a \, (t^a)_{ij} \; , \tag{2.4}$$

where A_μ^a is a real variable and ψ_α^a is a real Grassmann variable. We assume that the generators t^a are normalized as $\mathrm{tr}(t^a t^b) = \delta_{ab}$. The measure $\mathrm{d}\psi$ in (2.1) is defined by

$$\begin{aligned} \mathrm{d}\psi &= \prod_{\alpha=1}^{16} \prod_{a=1}^{N^2-1} \mathrm{d}\psi_\alpha^a \\ &= \prod_{\alpha=1}^{16} \left[\prod_{i<j} \{ 2 \, \mathrm{dRe}(\psi_\alpha)_{ij} \mathrm{dIm}(\psi_\alpha)_{ij} \} \prod_{i=1}^{N} \{ \mathrm{d}(\psi_\alpha)_{ii} \} \, \delta \left(\frac{1}{\sqrt{N}} \sum_{i=1}^{N} (\psi_\alpha)_{ii} \right) \right] \; , \end{aligned} \tag{2.5}$$

and similarly for dA. The model (2.1) appears after a Wick rotation, so that the metric has Euclidean signature. The 16×16 matrices $\tilde{\Gamma}_\mu$ are defined by

$$\tilde{\Gamma}_\mu = \mathcal{C}\,\Gamma_\mu \ , \tag{2.6}$$

where Γ_μ are ten-dimensional gamma matrices after Weyl projection, and the unitary matrix $\mathcal{C}$ is a charge conjugation matrix satisfying

$$\mathcal{C}\,\Gamma_\mu\,\mathcal{C}^\dagger = (\Gamma_\mu)^\top \quad ; \quad \mathcal{C}^\top = \mathcal{C} \ . \tag{2.7}$$

Due to (2.7), the matrices $\tilde{\Gamma}_\mu$ are symmetric.

An explicit representation of the gamma matrices is given by

$$\begin{aligned}
&\Gamma_1 = i\,\sigma_2 \otimes \sigma_2 \otimes \sigma_2 \otimes \sigma_2 \ ; \ \Gamma_2 = i\,\sigma_2 \otimes \sigma_2 \otimes \mathbf{1} \otimes \sigma_1 \ ; \ \Gamma_3 = i\,\sigma_2 \otimes \sigma_2 \otimes \mathbf{1} \otimes \sigma_3 \ ; \\
&\Gamma_4 = i\,\sigma_2 \otimes \sigma_1 \otimes \sigma_2 \otimes \mathbf{1} \ ; \ \Gamma_5 = i\,\sigma_2 \otimes \sigma_3 \otimes \sigma_2 \otimes \mathbf{1} \ ; \ \Gamma_6 = i\,\sigma_2 \otimes \mathbf{1} \otimes \sigma_1 \otimes \sigma_2 \ ; \\
&\Gamma_7 = i\,\sigma_2 \otimes \mathbf{1} \otimes \sigma_3 \otimes \sigma_2 \ ; \ \Gamma_8 = i\,\sigma_1 \otimes \mathbf{1} \otimes \mathbf{1} \otimes \mathbf{1} \ ; \ \Gamma_9 = i\,\sigma_3 \otimes \mathbf{1} \otimes \mathbf{1} \otimes \mathbf{1} \ ; \\
&\Gamma_{10} = \mathbf{1} \otimes \mathbf{1} \otimes \mathbf{1} \otimes \mathbf{1} \ ,
\end{aligned} \tag{2.8}$$

for which the charge conjugation matrix $\mathcal{C}$ becomes a unit matrix and therefore $\tilde{\Gamma}_\mu = \Gamma_\mu$.

The model has a manifest ten-dimensional Lorentz invariance, by which we actually mean an SO(10) invariance. A_μ transforms as a vector and ψ_α transforms as a Majorana-Weyl spinor. The model is manifestly supersymmetric, and also has a SU(N) symmetry

$$A_\mu \mapsto V A_\mu V^\dagger \quad ; \quad \psi_\alpha \mapsto V \psi_\alpha V^\dagger \ , \tag{2.9}$$

where $V \in$ SU(N). All these symmetries are inherited from the super Yang-Mills theory before taking the zero-volume limit. In particular, the SU(N) symmetry (2.9) is a remnant of the local gauge symmetry.

The fermion integral $Z_{\rm f}[A]$ in (2.1) can be obtained explicitly as

$$Z_{\rm f}[A] = {\rm Pf}\,\mathcal{M} \ , \tag{2.10}$$

where

$$\begin{aligned}
\mathcal{M}_{a\alpha,b\beta} &= -i\,\frac{1}{g^2}\,f_{abc}(\tilde{\Gamma}_\mu)_{\alpha\beta}A^c_\mu \ , \\
f_{abc} &= -i\,{\rm tr}(t^a[t^b,t^c]) \ .
\end{aligned} \tag{2.11}$$

The real totally-antisymmetric tensor f_{abc} gives the structure constants of SU(N) and the matrix $\mathcal{M}_{a\alpha,b\beta}$ is a $16\,(N^2-1) \times 16\,(N^2-1)$ anti-symmetric matrix, regarding each of $(a\alpha)$ and $(b\beta)$ as a single index.

The convergence of the integration over the bosonic matrices in (2.1) is nontrivial since the integration domain for the Hermitian matrices is non-compact. Even for finite N there is a potential danger of divergence when the eigenvalues of A_μ become large. This issue has been addressed in Ref. [23] using one-loop perturbative arguments which pointed to the finiteness of the IIB matrix model given by (2.1) for arbitrary N. This conclusion is in agreement with an exact result available for $N = 2$ [31] and a numerical result obtained for $N = 3$ [12]. Thus it is conceivable that the above conclusion, obtained by one-loop arguments, holds in general.

Since the model is well-defined without any cutoff, the parameter g, which is the only parameter of the model, can be absorbed by rescaling the variables,

$$A_\mu = g^{1/2} X_\mu \ , \tag{2.12}$$

$$\psi_\alpha = g^{3/4} \Psi_\alpha \ . \tag{2.13}$$

Therefore, g is a scale parameter rather than a coupling constant, i.e. the g dependence of physical quantities is completely determined on dimensional grounds[3]. In what follows, we take $g = 1$ without loss of generality.

For comparison, we also study the six-dimensional version of the IIB matrix model. In this regard we recall that pure $\mathcal{N} = 1$ supersymmetric Yang-Mills theory can be also defined in 3D, 4D and 6D, as well as in 10D. Hence, by taking a zero-volume limit of these theories, we arrive at supersymmetric large N reduced models which are $D = 3, 4, 6$ versions of the IIB matrix model. Using the one-loop argument mentioned above, one concludes that the model is ill-defined for $D = 3$, but well-defined for $D = 4, 6, 10$, irrespectively of N. For $D = 4$, Monte Carlo simulations up to $N = 48$ further confirms this statement [18]. The effective action induced by fermions (logarithm of the fermion integral $Z_{\rm f}[A]$) is real for $D = 4$. It is complex in general for $D = 6$ and $D = 10$, however, which causes the sign problem in Monte Carlo simulations.

[3]The scale parameter g should be tuned appropriately as one sends N to infinity so that all the correlation functions of Wilson loops have a finite large N limit. Whether such a limit really exists or not is one of the important dynamical issues, which was addressed in Ref. [18] for the four-dimensional version of the IIB matrix model.

3 Low-energy effective theory

In this section, we derive the low-energy effective theory of the IIB matrix model (2.1) along the lines discussed in Ref. [23]. We first decompose the $N \times N$ Hermitian matrices A_μ and ψ_α as

$$\begin{aligned} A_\mu &= \hat{x}_\mu + \hat{a}_\mu \ , \\ \psi_\alpha &= \hat{\xi}_\alpha + \hat{\varphi}_\alpha \ , \end{aligned} \tag{3.1}$$

where $\hat{x}_\mu$ and $\hat{\xi}_\alpha$ represent the diagonal parts, while $\hat{a}_\mu$ and $\hat{\varphi}_\alpha$ represent the off-diagonal parts. We also introduce N ten-dimensional vectors x_i $(i = 1, \cdots, N)$ through $x_{i\mu} = (\hat{x}_\mu)_{ii}$, and N ten-dimensional Majorana-Weyl spinors ξ_i $(i = 1, \cdots, N)$ through $\xi_{i\alpha} = (\hat{\xi}_\alpha)_{ii}$. For the off-diagonal elements, we use the notations $a_{\mu ij} = (\hat{a}_\mu)_{ij}$ and $\varphi_{\alpha ij} = (\hat{\varphi}_\alpha)_{ij}$, where $i \neq j$. Using the decomposition (3.1), the actions (2.2) and (2.3) can be written as

$$S_{\rm b} = -{\rm tr}\left(-\frac{1}{2}\hat{a}_\nu [\hat{x}_\mu, [\hat{x}_\mu, \hat{a}_\nu]] - \frac{1}{2}[\hat{x}_\mu, \hat{a}_\mu]^2 + [\hat{x}_\mu, \hat{a}_\nu][\hat{a}_\mu, \hat{a}_\nu] + \frac{1}{4}[\hat{a}_\mu, \hat{a}_\nu]^2 \right) \ , \tag{3.2}$$

$$S_{\rm f} = -\frac{1}{2}\,(\tilde{\Gamma}_\mu)_{\alpha\beta}\,{\rm tr}\Big(\hat{\varphi}_\alpha [\hat{x}_\mu, \hat{\varphi}_\beta] - \hat{\varphi}_\alpha [\hat{\xi}_\beta, \hat{a}_\mu] - \hat{a}_\mu [\hat{\xi}_\alpha, \hat{\varphi}_\beta] + \hat{\varphi}_\alpha [\hat{a}_\mu, \hat{\varphi}_\beta] \Big) \ . \tag{3.3}$$

The one-loop approximation amounts to keeping only the quadratic terms in a and φ in the above expressions, neglecting the higher-order terms, i.e., the $\mathrm{O}(a^3)$ term and the $\mathrm{O}(a^4)$ term in $S_{\rm b}$ and the $\mathrm{O}(a\varphi^2)$ term in $S_{\rm f}$. The quadratic term in a in (3.2) has zero modes due to the fact that the original model (2.1) has the SU(N) invariance (2.9). We thus have to "fix the gauge" properly. Following Ref. [23], we choose the "gauge-fixing" term (which is the reduced model counterpart of the Feynman gauge in ordinary gauge theory) and the corresponding Faddeev-Popov ghost term as

$$\begin{aligned} S_{\rm g.f.} &= -\frac{1}{2}{\rm tr}([\hat{x}_\mu, \hat{a}_\mu]^2) \ , \\ S_{\rm gh} &= -{\rm tr}([\hat{x}_\mu, \hat{b}][\hat{x}_\mu + \hat{a}_\mu, \hat{c}]) \ . \end{aligned} \tag{3.4}$$

$\hat{a}_\mu$ in the ghost action $S_{\rm gh}$ can be neglected within the one-loop approximation. Integration over the ghost fields $\hat{b}$, $\hat{c}$ then yields $\{\Delta(x)\}^2$, where $\Delta(x)$ is defined as

$$\Delta(x) = \prod_{i<j} (x_i - x_j)^2 \ . \tag{3.5}$$

Therefore, the partition function at the one-loop approximation can be written as

$$Z_{\rm IIB}^{(1-{\rm loop})} = \int {\rm d}x\, {\rm d}a\, {\rm e}^{-S_{\rm G}}\, \{\Delta(x)\}^2\, Z_{\rm f}^{(1-{\rm loop})}[x, a] \ , \tag{3.6}$$

where

$$S_{\rm G} = \sum_{i<j} (x_i - x_j)^2 |a_{\mu ij}|^2 \ , \tag{3.7}$$

and the one-loop approximated fermion integral is defined as

$$Z_{\rm f}^{(1-{\rm loop})}[x,a] = \int {\rm d}\xi \, {\rm d}\varphi \ {\rm e}^{-S_{\rm f}^{(2)}} \ , \tag{3.8}$$

$$S_{\rm f}^{(2)} = -\frac{1}{2} (\tilde{\Gamma}_\mu)_{\alpha\beta} {\rm tr} \Big(\hat{\varphi}_\alpha [\hat{x}_\mu, \hat{\varphi}_\beta] - \hat{\varphi}_\alpha [\hat{\xi}_\beta, \hat{a}_\mu] - \hat{a}_\mu [\hat{\xi}_\alpha, \hat{\varphi}_\beta] \Big) \ . \tag{3.9}$$

In what follows we calculate $Z_{\rm f}^{(1-{\rm loop})}[x,a]$ explicitly. We first note that $S_{\rm f}^{(2)}$ can be written as

$$S_{\rm f}^{(2)} = -\frac{1}{2} \sum_{i \neq j} \tilde{\varphi}_{\alpha j i} (\tilde{\Gamma}_\mu)_{\alpha\beta} (x_{i\mu} - x_{j\mu}) \tilde{\varphi}_{\beta i j} - \frac{1}{2} \sum_{ij} \xi_{i\alpha} M'_{i\alpha, j\beta} \xi_{j\beta} \ , \tag{3.10}$$

where $\tilde{\varphi}_{\alpha ij}$ in (3.10) are defined by

$$\tilde{\varphi}_{\alpha ij} = \varphi_{\alpha ij} - \frac{(x_{i\rho} - x_{j\rho})}{(x_i - x_j)^2} (\tilde{\Gamma}_\rho^\dagger \tilde{\Gamma}_\sigma)_{\alpha\beta} a_{\sigma ij} (\xi_{i\beta} - \xi_{j\beta}) \ , \tag{3.11}$$

and $M'_{i\alpha, j\beta}$ is a $16N \times 16N$ matrix given as

$$M'_{i\alpha, j\beta} = \frac{(x_{i\rho} - x_{j\rho})}{(x_i - x_j)^2} (\tilde{\Gamma}_\mu \tilde{\Gamma}_\rho^\dagger \tilde{\Gamma}_\sigma)_{\alpha\beta} (a_{\mu ji} a_{\sigma ij} - a_{\mu ij} a_{\sigma ji}) \qquad \text{for} \quad i \neq j \ , \tag{3.12}$$

$$M'_{i\alpha, i\beta} = -\sum_{j \neq i} M'_{i\alpha, j\beta} \ . \tag{3.13}$$

Integration over $\tilde{\varphi}$ can now be done yielding $\{\Delta(x)\}^8$. We then integrate out $\xi_{N\alpha}$ using the delta functions in (2.5), yielding a factor of $1/N^8$ followed by a replacement

$$\xi_{N\alpha} \Rightarrow -\sum_{j=1}^{N-1} \xi_{j\alpha} \tag{3.14}$$

in (3.10). The integration over the $\xi_{i\alpha}$ $(i = 1, \cdots, (N-1))$ yields ${\rm Pf}\, M$. The matrix M is a $16(N-1) \times 16(N-1)$ complex matrix defined as

$$M_{i\alpha, j\beta} = M'_{i\alpha, j\beta} - M'_{N\alpha, j\beta} - M'_{i\alpha, N\beta} + M'_{N\alpha, N\beta} \ , \tag{3.15}$$

where indices i and j run from 1 to $N-1$. Note that there are identities

$$M'_{j\alpha, i\beta} = M'_{i\alpha, j\beta} \quad , \quad M'_{i\beta, j\alpha} = -M'_{i\alpha, j\beta} \ , \tag{3.16}$$

and similarly for $M_{i\alpha, j\beta}$. This means in particular that $M_{i\alpha, j\beta}$ is an anti-symmetric matrix, regarding each of $(i\alpha)$ and $(j\beta)$ as a single index. Thus the one-loop approximated fermion integral is obtained as

$$Z_{\rm f}^{(1-{\rm loop})}[x,a] = \{\Delta(x)\}^8 \frac{1}{N^8} {\rm Pf}\, M \ . \tag{3.17}$$

We have checked numerically that indeed

$$Z_{\rm f}[A] \simeq Z_{\rm f}^{(1-\text{loop})}[x,a] \quad ; \quad (A_\mu)_{ij} = x_{i\mu}\,\delta_{ij} + a_{\mu ij} \ , \tag{3.18}$$

holds when the x_i's are well-separated and $a_{\mu ij}$ are generated with the distribution $\mathrm{e}^{-S_{\rm G}}$, where $S_{\rm G}$ is given by (3.7). Note that the size of the matrix M in (3.17) is of $\mathrm{O}(N)$, whereas the size of the matrix $\mathcal{M}$ in (2.10) is of $\mathrm{O}(N^2)$. The huge reduction is essentially because the integration over the fermionic off-diagonal elements has been done explicitly yielding $\{\Delta(x)\}^8$ in (3.17). This is the substantial gain from using the one-loop approximation.

First we note that the model (3.6) as it stands has a singularity[4] at $x_{i\mu} = 0$ due to the singularity in (3.12). Therefore if one simulates the model (3.6), the distribution of x_i collapses to the origin. We recall that such an ultraviolet singularity does not exist in the original IIB matrix model. On the other hand, the one-loop approximation is valid only when x_i's are well separated from each other. Therefore, we have to introduce a UV cutoff to the distribution of x_i in order to make the model meaningful. As a UV cutoff, we introduce in the action the term given as

$$S_{\rm cut} = \sum_{i<j} f(\sqrt{(x_i - x_j)^2}) \ , \tag{3.19}$$

where the function $f(x)$ is taken to be

$$f(r) = \begin{cases} \frac{\kappa}{2\ell^2}(r-\ell)^2 & \text{for} \quad r < \ell \\ 0 & \text{for} \quad r \geq \ell \ . \end{cases} \tag{3.20}$$

The dimensionless "spring constant" κ should be taken to be large enough to prevent the x_i's from coming closer to each other than the cutoff ℓ (See Figs. 1 and 2.). Thus we arrive at the low-energy effective theory of the IIB matrix model (2.1)

$$Z_{\rm LEET} = \int \mathrm{d}x\, \mathrm{d}a\, \mathrm{e}^{-S_{\rm G} - S_{\rm cut}}\, \{\Delta(x)\}^{10}\, \mathrm{Pf}\, M \ , \tag{3.21}$$

which is written in terms of bosonic variables only. We have omitted the irrelevant constant factor $\frac{1}{N^8}$ in (3.17).

In fact, the UV cutoff parameter ℓ can be scaled away from the theory (3.21) by rescaling the variables as $x_{i\mu} \mapsto \ell x_{i\mu}$ and $a_{\mu ij} \mapsto \frac{1}{\ell} a_{\mu ij}$. This means that the dependence of the results on the UV cutoff ℓ is determined completely on dimensional grounds. In particular,

[4] This can be seen more clearly by rescaling $a_{\mu ij}$ as in (A.1). Then, one finds that all the $x_{i\mu}$-dependence of the partition function is contained in the Pfaffian, which has the singularity.

dimensionless quantities are independent of ℓ. When we are interested in dimensionful quantities, and in particular in their large N behavior, we have to know the N-dependence of the UV cutoff ℓ. In Ref. [23], it was argued that ℓ should be taken to be N-independent, based on a reasonable assumption that the ultraviolet behavior of the space-time structure of the IIB matrix model is controlled by the SU(2) matrix model. The issue is also addressed in the four-dimensional version of the IIB matrix model in Ref. [18]. There, an N-independent UV cutoff was shown to be generated dynamically by treating the full model nonperturbatively instead of making perturbative expansions around diagonal matrices. We therefore take $\ell = 1$ for all N in the following.

The Pfaffian $\mathrm{Pf}\, M$ in (3.21) is complex in general. This poses the notorious "sign problem", when one tries to study the model by Monte Carlo simulation. Note, however, that the problem is simply inherited from the original IIB matrix model (2.1), as can be seen from (3.18). In the present work, we take the absolute value $|\mathrm{Pf}\, M|$ and throw away the phase by hand. This corresponds to taking the absolute value $|\mathrm{Pf}\, \mathcal{M}|$ of the Pfaffian in the IIB matrix model and studying its low-energy effective theory.

To summarize, the model we simulate is given by the partition function

$$Z = \int \mathrm{d}x \, \mathrm{d}a \, \mathrm{e}^{-S_{\mathrm{G}} - S_{\mathrm{cut}}} \, \{\Delta(x)\}^{10} \, |\mathrm{Pf}\, M| \ . \tag{3.22}$$

S_{G} and S_{cut} are given by (3.7) and (3.19) respectively, and M is defined through (3.12), (3.13) and (3.15). Note that the model (3.22) still has the 10D Lorentz invariance. We would like to investigate whether the 10D Lorentz invariance breaks down, say, to 4D Lorentz invariance. The model corresponding to the six-dimensional version of the IIB matrix model can be obtained similarly.

The validity of the one-loop approximation for studying the low-energy dynamics of supersymmetric large N reduced models has been addressed in Ref. [18] by studying the four-dimensional version of the IIB matrix model without any approximations. It was found that the large N behavior of the extent of the distribution of x_i agrees with the prediction from the one-loop, low-energy effective theory. We therefore expect that a low-energy phenomenon such as SSB of Lorentz invariance can be studied with the low-energy effective theory.

On the other hand we note that from a technical point of view the one-loop approximation offers certain advantages which are essential in the present work. We recall that even in the four-dimensional version of the IIB matrix model, the largest N one can achieve for the full model (without the one-loop approximation) is $N = 48$ using supercomputers. In order

to detect even a small trend of SSB of Lorentz invariance from 10D to 4D, say, one would expect that N should be larger than $4^4 = 256$. Due to the fact that the size of the matrix M in (3.22) is order of N smaller than the size of the matrix $\mathcal{M}$ in (2.10), the one-loop approximation enables us to reach $N = 512$ with reasonable effort. Details of the algorithm used in the Monte Carlo simulations are presented in the Appendix A. The algorithm is a variant of the Hybrid Monte Carlo algorithm [26] which is one of the standard algorithms used in the study of systems with dynamical fermions. The computational effort of the algorithm is estimated to be $\mathrm{O}(N^3)\sim\mathrm{O}(N^{7/2})$, which should be compared with an estimate $\mathrm{O}(N^5)$ for the algorithm used for the full model in Ref. [18].

4 Results for the distribution of x_i

First we look at the distribution $\rho(r)$ of the distance r between x_i's, where the distance between two arbitrary points $x_i \neq x_j$ is measured by $\sqrt{(x_i - x_j)^2}$. In Fig. 1, we plot the results for $D = 10$ with $N = 192$, 256, 384 and 512. Fig. 2 shows the results for $D = 6$ with $N = 256$, 512 and 768. We note that in both cases the distribution at small r falls off rapidly below $r \sim \ell$, where $\ell = 1$ is the UV cutoff introduced in (3.20). The small penetration into the $r < \ell$ region is due to κ being finite. However, the results show that the values of κ we have taken ($\kappa = 300$ for $D = 10$ and $\kappa = 100$ for $D = 6$) are large enough to make the penetration reasonably small.

In order to see the spontaneous breakdown of Lorentz invariance, we consider the moment of inertia tensor of N points x_i $(i = 1, \cdots, N)$ in a flat D-dimensional space-time[5] . It can be defined as

$$T_{\mu\nu} = \frac{2}{N(N-1)} \sum_{i<j} (x_{i\mu} - x_{j\mu})(x_{i\nu} - x_{j\nu}) \ , \tag{4.1}$$

which is a $D \times D$ real symmetric matrix. The D eigenvalues $\lambda_1 > \lambda_2 > \cdots > \lambda_D > 0$ of the matrix T represent the principal moments of inertia. We measure λ_μ for each configuration and take an average $\langle \lambda_\mu \rangle$ over all the configurations generated by the Monte Carlo simulation. If Lorentz invariance is not spontaneously broken, $\langle \lambda_\mu \rangle$ must be all equal in the large N limit, representing an isotropic distribution of x_i. We therefore search for a trend which differs from such a large N behavior.

[5]Such a quantity has also been studied in Refs. [14, 23].

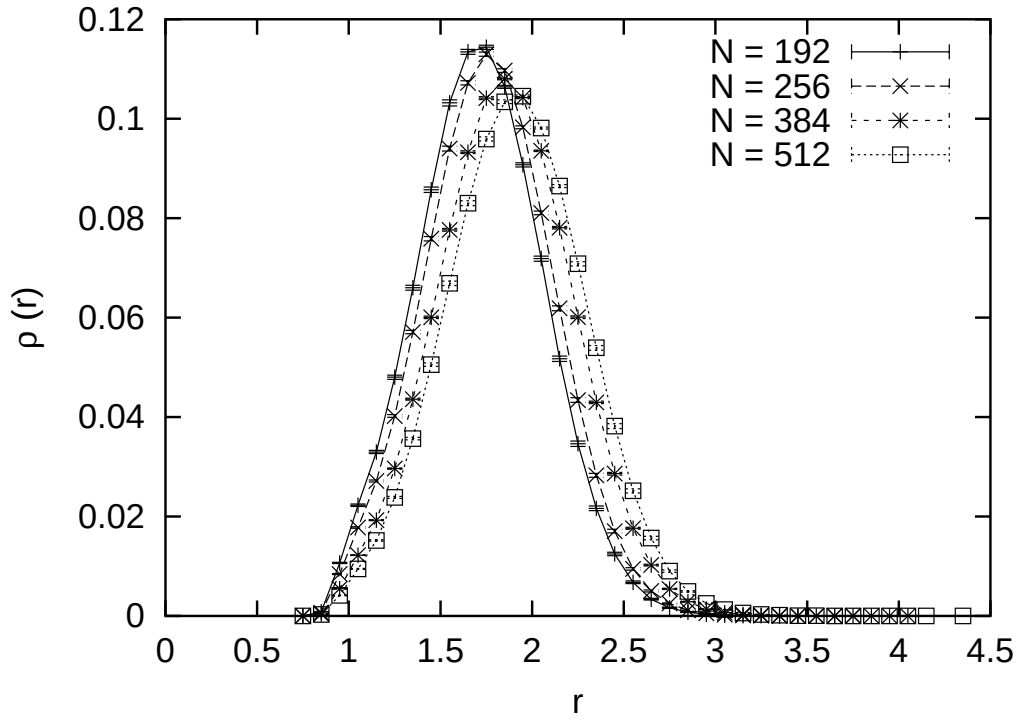

Figure 1: The distribution of distances $\rho(r)$ for $D = 10$ is plotted against r for $N = 192$, 256, 384 and 512.

We first note that if the system that describes the dynamics of x_i were a simple branched polymer in a flat D-dimensional space-time, spontaneous breakdown of Lorentz invariance would certainly not occur, and moreover, the large N behavior of $\langle\lambda_\mu\rangle$ could be expected to be $\langle\lambda_\mu\rangle \sim N^{1/2}$. This is due to the fact that the Hausdorff dimension of a branched polymer is $d_{\rm H} = 4$ irrespectively of the dimension D of the space-time in which it is embedded. For this we note that the extent of the distribution of x_i is given by

$$R = \sqrt{T_{\mu\mu}} = \sqrt{\sum_{\mu=1}^{D} \lambda_\mu} \ , \tag{4.2}$$

which is related to the number N of points through $N \sim (R/\ell)^{d_{\rm H}}$. The ℓ is the UV cutoff taken to be $\ell = 1$. Therefore, we find $R \sim N^{1/d_{\rm H}} \sim N^{1/4}$, which leads to the announced large N behavior $\langle\lambda_\mu\rangle \sim N^{1/2}$.

In Fig. 3 we plot the normalized eigenvalues $\langle\lambda_\mu\rangle/N^{1/2}$ against $1/N$ for $D = 10$ with $N = 192, 256, 384, 512$. We find that the smallest (normalized) eigenvalue $\langle\lambda_{10}\rangle/N^{1/2}$ is almost constant and the larger ones are monotonously decreasing towards the same constant. Thus the observed large N behavior suggests that there is *no* spontaneous breakdown of Lorentz

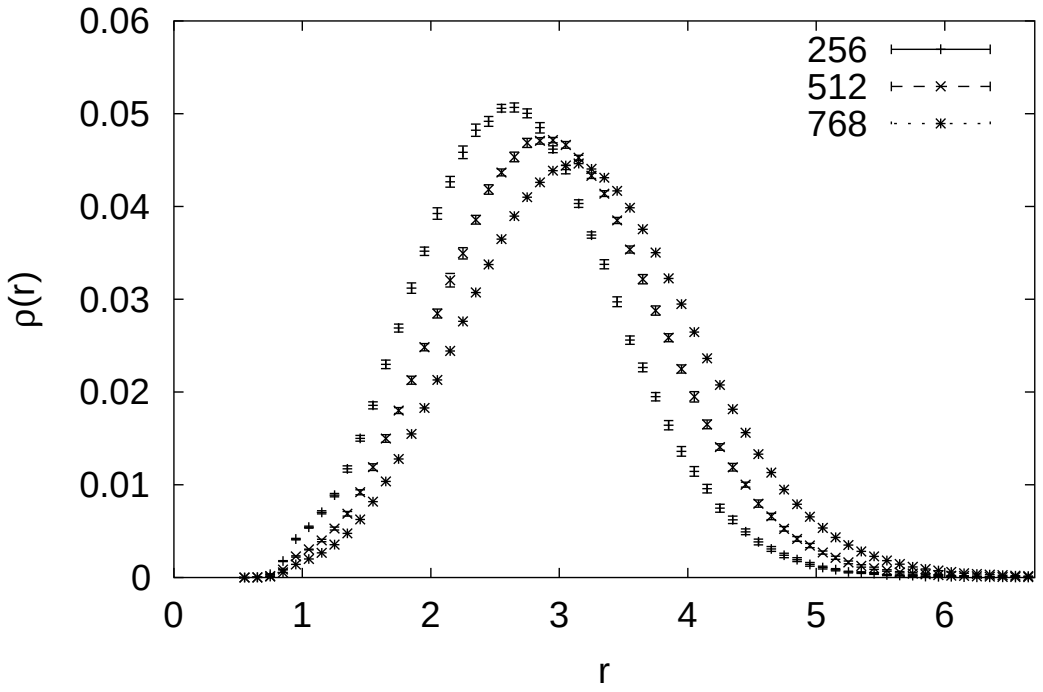

Figure 2: The distribution of distances $\rho(r)$ for $D = 6$ is plotted against r for $N = 256$, 512 and 768.

invariance and the large N behavior of the extent of the x-distribution is consistent with a simple branched-polymer prediction. In particular, we see no trend for a gap developing between the fourth and the fifth largest eigenvalues, which could have been observed if the 10D Lorentz invariance were broken down to a four-dimensional one. In Fig. 4 we present the results for $D = 6$ with $N = 192, 256, 512, 768$. The qualitative behavior is the same as in $D = 10$.

The results for $D = 10$ might suggest that the leading finite N effect is given by $1/N$. For example, a linear extrapolation in $1/N$ using the data for $N = 384, 512$ leads to almost the same results for all the ten (normalized) eigenvalues at $N = \infty$. It is therefore tempting to speculate that finite N effects in the IIB matrix model is given by a $1/N$ expansion. Such a form of finite N effects, if it is true, is in remarkable contrast to the "bosonic" case, in which the fermions in the IIB matrix model (2.1) is omitted by hand. In that case, the large N behavior of correlation functions was determined analytically [14] to all orders in the $1/D$ expansion and finite N effects were found to be given by a $1/N^2$ expansion.

For $D = 6$, the linear extrapolation gives almost the same results up to the third smallest eigenvalue, but not for the larger ones. Thus, as far as reproducing an isotropic distribution

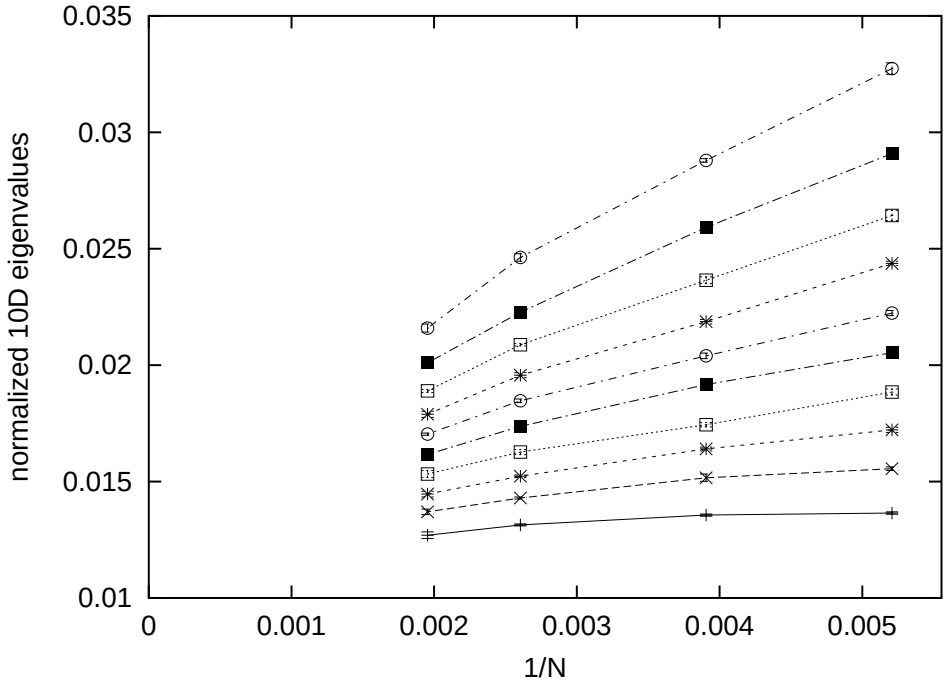

Figure 3: The 10 eigenvalues of the moment of inertia tensor normalized by $N^{1/2}$ are plotted against $1/N$ for $N = 192, 256, 384, 512$.

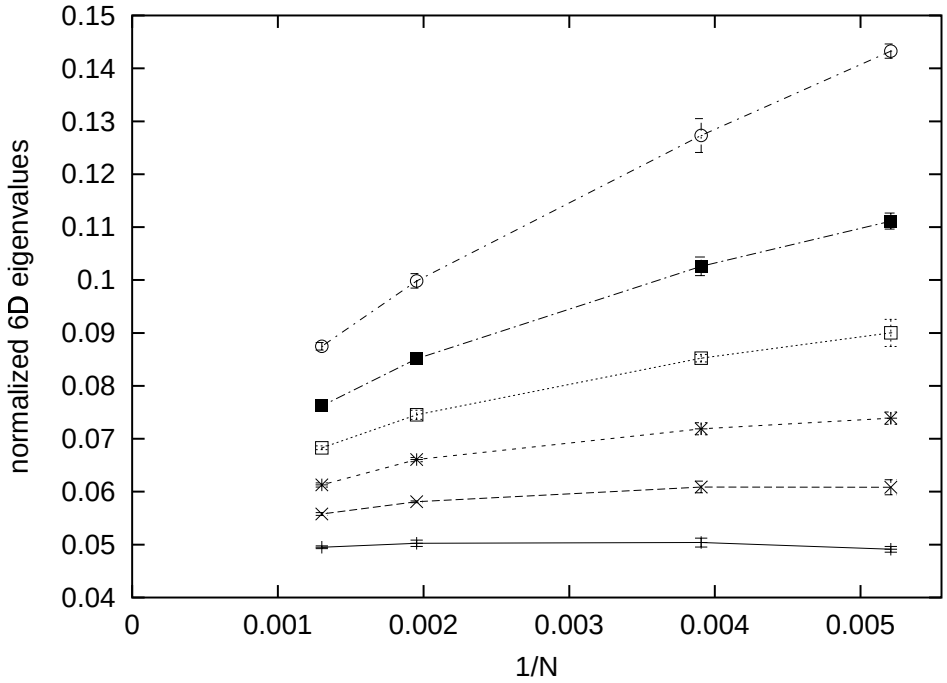

Figure 4: The 6 eigenvalues of the moment of inertia tensor normalized by $N^{1/2}$ are plotted against $1/N$ for $N = 192, 256, 512, 768$.

of x_i in the large N limit is concerned, $D = 6$ seems to have larger finite N effects. This rather counter-intuitive result might be understood by considering the branched-polymer representation of the low-energy effective theory [23]. The attractive potential between two x_i's connected by a bond is given by $r^{-3(D-2)}$, where $r = \sqrt{(x_i - x_j)^2}$. Therefore, it is much stronger for $D = 10$ than for $D = 6$. Since the branched-polymer system in both cases is not a simple maximal tree but something more complicated, typically involving a double-tree structure, it may well be that the stronger the attractive potential is, the more the distribution of x_i tends to become isotropic.

5 Summary and Discussion

In this paper, we studied the IIB matrix model (and its six-dimensional version) at large N by using the low-energy effective theory developed in Ref. [23]. Unlike in the four-dimensional version studied in Ref. [18], the fermion integral yields a Pfaffian (or a determinant in the 6D case) which is complex in general. In the present paper we omitted the phase of the Pfaffian by hand in order to avoid the sign problem in the Monte Carlo simulations, and we studied the effect of the modulus only. We have seen that the distribution of x_i becomes more and more isotropic as we increase N. Based on this observation we conclude that if the SSB ever occurs in the original IIB matrix model, the phase of the Pfaffian induced by fermions must play a crucial rôle.

It is interesting to compare with the situation in perturbative superstring theory. Also in that case the fermionic degrees of freedom can be integrated out explicitly [27], leaving us with an effective bosonic string theory, where the action consists of three parts: the ordinary bosonic string action, an extrinsic curvature term, and (in Euclidean space-time) a purely imaginary Wess-Zumino-like term. This means that if we can neglect the imaginary part, the superstring theory is equivalent to a bosonic string theory with extrinsic curvature. While this equivalence has not been directly disproved, it does not have much support, either, from numerical simulations and analytical calculations [20, 28, 29].

In Ref. [30] a deformation of the IIB matrix model by introducing an integer parameter ν which couples to the phase of the Pfaffian has been considered. The original IIB matrix model corresponds to $\nu = 1$. The deformed model continues to be well-defined, and preserves Lorentz invariance, the SU(N) symmetry, and the cluster property. In this language the

present work corresponds to the study of the case $\nu = 0$ using the low-energy effective theory. The opposite extreme, the limit $\nu = \infty$, has been studied analytically in Ref. [30], and the spontaneous breakdown of Lorentz invariance has been discovered. Of particular interest is the fact that different conclusions have been obtained for $\nu = \infty$ and for $\nu = 0$, which already implies that a phase transition should occur in between. If the original IIB matrix model ($\nu = 1$) belongs to the same phase as $\nu = \infty$, we can investigate the dynamics of the IIB matrix model by studying the $\nu = \infty$ model using Monte Carlo simulation as suggested in Ref. [30]. It would be extremely interesting if we can obtain a flat four-dimensional spacetime in that way. We hope that the Monte Carlo technique developed in the present work is useful for such future studies and eventually enables us to explore the dynamics of the IIB matrix model.

Acknowledgments

We would like to thank R.J. Szabo and G. Vernizzi for carefully reading the manuscript. J. A. and K.N. A. acknowledge the support of MaPhySto — Centre for Mathematical Physics and Stochastics, funded by the Danish National Research Foundation. K.N. A. acknowledges partial support from a postdoctoral fellowship from the Greek Institute of National Fellowships (IKY). J. N. is supported by the Japan Society for the Promotion of Science as a Postdoctoral Fellow for Research Abroad. The computation has been carried out on VPP500 at High Energy Accelerator Research Organization (KEK), VPP700E at The Institute of Physical and Chemical Research (RIKEN), SR8000 at Computer Centre, University of Tokyo, and SX4 at Research Center for Nuclear Physics (RCNP) of Osaka University. J. N. is grateful to T. Ishikawa, S. Ohta, A.I. Sanda, H. Toki, S. Uehara and Y. Watanabe for many kind helps in using the supercomputers. This work is supported by the Supercomputer Project (No.99-53) of KEK.

Appendix A: The algorithm for the simulation

In this appendix, we explain the algorithm[6] we use for the Monte Carlo simulation of our model defined by (3.22).

We first simplify the model by introducing rescaled variables $b_{\mu ij}$ as

$$b_{\mu ij} = \sqrt{(x_i - x_j)^2}\, a_{\mu ij} \ . \tag{A.1}$$

The model we have to simulate then becomes

$$Z = \int \mathrm{d}x\, \mathrm{d}b\, \mathrm{e}^{-S_{\mathrm{G}} - S_{\mathrm{cut}}} \left| \mathrm{Pf}\, M \right| \ , \tag{A.2}$$

where

$$S_{\mathrm{G}} = \sum_{i<j} |b_{\mu ij}|^2 \ , \tag{A.3}$$

and (3.12) can be rewritten in terms of b_{ij} as

$$M'_{i\alpha,j\beta} = \frac{(x_{i\rho} - x_{j\rho})}{\{(x_i - x_j)^2 + (\epsilon\ell)^2\}^2} (\tilde{\Gamma}_\mu \tilde{\Gamma}^\dagger_\rho \tilde{\Gamma}_\sigma)_{\alpha\beta} (b_{\mu ji} b_{\sigma ij} - b_{\mu ij} b_{\sigma ji}) \qquad \text{for} \quad i \neq j \ , \tag{A.4}$$

where we have also introduced the dimensionless regularization parameter ϵ to reduce numerical instabilities. The regularization parameter ϵ should be taken to be small enough not to affect the system. For both, 6D and 10D, cases, we took $\epsilon = 0.1$. We note also that with this regularization, the model is well-defined without introducing the cutoff term (3.19). However, by simulating such a model, we find that all the x_i's become densely packed within the extent $\epsilon\ell$ as we increase N. Therefore, we still need the cutoff term (3.19) in order to make our model valid as a low-energy effective theory of the original IIB matrix model. For convenience we combine our dynamical variables $x_{i\mu}$ and $b_{\mu ij}$ ($i \neq j$, $b_{\mu ji} = b^*_{\mu ij}$) into a Hermitian matrix B_μ as $(B_\mu)_{ij} = x_{i\mu}\, \delta_{ij} + b_{\mu ij}$.

The algorithm we use to simulate the model (A.2) is a variant of the Hybrid Monte Carlo algorithm [26]. The first step of the Hybrid Monte Carlo algorithm is to apply molecular dynamics [33]. We introduce a conjugate momentum for $B_{\mu ij}$ as $X_{\mu ij}$, which satisfies $X_{\mu ji} =$

[6] Ref. [32] gives an overview of effective algorithms for dynamical fermions.

$(X_{\mu ij})^*$; X_μ are Hermitian matrices. The partition function can be rewritten as[7]

$$Z = \int \mathrm{d}X \, \mathrm{d}B \, \mathrm{e}^{-H} \ , \tag{A.5}$$

where H is the "Hamiltonian" defined by

$$H = \frac{1}{2} \sum_{\mu ij} |X_{\mu ij}|^2 + S_{\mathrm{G}}[B] + S_{\mathrm{cut}}[B] - \frac{1}{2} \ln |\det M| \ . \tag{A.6}$$

The update of $X_{\mu ij}$ can be done by just generating $X_{\mu ij}$ with the probability distribution $\exp(-\frac{1}{2}\sum |X_{\mu ij}|^2)$. In order to update $B_{\mu ij}$, we solve the Hamilton equation given by

$$\frac{\mathrm{d}B_{\mu ij}(\tau)}{\mathrm{d}\tau} = \frac{\partial H}{\partial X_{\mu ij}} = X_{\mu ji} \tag{A.7}$$

$$\frac{\mathrm{d}X_{\mu ij}(\tau)}{\mathrm{d}\tau} = -\frac{\partial H}{\partial B_{\mu ij}} = \frac{1}{4}\mathrm{Tr}\left(\frac{\partial D}{\partial B_{\mu ij}} D^{-1}\right) - \frac{\partial S_{\mathrm{G}}}{\partial B_{\mu ij}} - \frac{\partial S_{\mathrm{cut}}}{\partial B_{\mu ij}} \ , \tag{A.8}$$

where we have defined $D = M^\dagger M$. Note that when taking the derivatives in (A.8), $(B_\mu)_{ij}$ and $(B_\mu)_{ji}$ should be treated as independent complex variables. Along the "classical trajectory" given by the Hamilton equation,

(i) H is invariant,

(ii) the motion is reversible,

(iii) the phase-volume is preserved; *i.e.*

$$\frac{\partial(B(\tau), X(\tau))}{\partial(B(0), X(0))} = 1 \ , \tag{A.9}$$

where $(B(\tau), X(\tau))$ is the point on the trajectory after evolution for fixed τ from $(B(0), X(0))$. Therefore, generating a new sets of (B, X) by solving the Hamilton equation for a fixed "time" interval τ satisfies the detailed balance. This procedure, together with the proceeding generation of $X_{\mu ij}$ with the Gaussian distribution, is called "one trajectory", which corresponds to "one sweep" in ordinary Monte Carlo simulations.

When solving the Hamilton equation numerically, we have to discretize the equation. A discretization which preserves the properties (ii) and (iii) is known. The property (i) cannot be preserved and yields a small violation of the Hamiltonian conservation. In order to still

[7] Unlike in the standard Hybrid Monte Carlo algorithm [26], we do not introduce the so-called pseudo-fermions. Note, in this regard, that our system (A.2) is different from ordinary field theories with dynamical fermions in the following respects. 1) The number of fermion flavors should be strictly one in order to respect supersymmetry. 2) The size of the matrix M is much smaller than the system size. 3) The matrix M is not sparse.

satisfy the detailed balance exactly, we can perform a Metropolis accept/reject as the end of each trajectory.

We introduce a short-hand notation for discretized $X_\mu(\tau)$ and $B_\mu(\tau)$ as

$$X_\mu^{(r)} = X_\mu(r\Delta\tau) \quad ; \qquad B_\mu^{(s)} = B_\mu(s\Delta\tau) \ . \tag{A.10}$$

Given the configuration $(B_\mu^{(0)}, X_\mu^{(0)})$, the configuration $(B_\mu^{(\nu)}, X_\mu^{(\nu)})$ after the evolution for a fixed time $\tau = \nu\,\Delta\tau$ is obtained by solving the discretized Hamilton equation

$$\begin{aligned}
B_{\mu ij}^{(\frac{1}{2})} &= B_{\mu ij}^{(0)} + \frac{\Delta\tau}{2} X_{\mu ji}^{(0)} \\
B_{\mu ij}^{(n+\frac{1}{2})} &= B_{\mu ij}^{(n-\frac{1}{2})} + \Delta\tau X_{\mu ji}^{(n)} \\
B_{\mu ij}^{(\nu)} &= B_{\mu ij}^{(\nu-\frac{1}{2})} + \frac{\Delta\tau}{2} X_{\mu ji}^{(\nu)} \qquad \text{(A.11)} \\
X_{\mu ij}^{(m+1)} &= X_{\mu ij}^{(m)} - \Delta\tau \frac{\partial H}{\partial B_{\mu ij}}(B_\mu^{(m+\frac{1}{2})}) \ , \qquad \text{(A.12)}
\end{aligned}$$

where $n = 1, 2, \cdots, \nu-1$ and $m = 0, 1, \cdots, \nu-1$. Note that the first and the final steps in the evolution (A.11) of B_μ are treated with special care. This particular discretization, which is called as "leap-frog discretization", preserves the properties (ii) and (iii). At the end of the trajectory, we make a Metropolis accept/reject with the probability $P = \min(1, \mathrm{e}^{-\Delta H})$, where ΔH is the difference of the Hamiltonian H defined in (A.6) for the configurations $(B_\mu^{(0)}, X_\mu^{(0)})$ and $(B_\mu^{(\nu)}, X_\mu^{(\nu)})$. Optimization of $\Delta\tau$ and ν is discussed in Appendix B.

In the evolution (A.12) of X_μ, one needs to calculate

$$\mathrm{Tr}\left(\frac{\partial D}{\partial B_{\mu ij}} D^{-1}\right) = \mathrm{Tr}\left(\frac{\partial M}{\partial B_{\mu ij}} M^{-1}\right) + \mathrm{Tr}\left(\frac{\partial M^\dagger}{\partial B_{\mu ij}} M^{\dagger -1}\right) \ . \tag{A.13}$$

If we write the first term as $T_{\mu ij}$, the second term can be written as $T^*_{\mu ji}$. In what follows, we calculate $T_{\mu ij}$ explicitly. We first note that

$$T_{\mu ij} = \sum_{k,l=1}^{N-1} \sum_{\alpha\beta} \frac{\partial M_{k\alpha,l\beta}}{\partial B_{\mu ij}} C_{l\beta,k\alpha} = \sum_{k,l=1}^{N} \sum_{\alpha\beta} \frac{\partial M'_{k\alpha,l\beta}}{\partial B_{\mu ij}} C'_{l\beta,k\alpha} \ , \tag{A.14}$$

where $C_{i\alpha,j\beta}$ is defined as

$$C_{i\alpha,j\beta} = (M^{-1})_{i\alpha,j\beta} \ , \tag{A.15}$$

and $C'_{i\alpha,j\beta}$ is defined as

$$\begin{aligned}
C'_{i\alpha,j\beta} &= C_{i\alpha,j\beta} \quad ; \quad C'_{i\alpha,N\beta} = -\sum_{k=1}^{N-1} C_{i\alpha,k\beta} \\
C'_{N\alpha,j\beta} &= -\sum_{k=1}^{N-1} C_{k\alpha,j\beta} \quad ; \quad C'_{N\alpha,N\beta} = \sum_{k,l=1}^{N-1} C_{k\alpha,l\beta} \ . \qquad \text{(A.16)}
\end{aligned}$$

The indices i, j in (A.15) and (A.16) run from 1 to $N-1$. We further rewrite $T_{\mu ij}$ as

$$T_{\mu ij} = \sum_{k=1}^{N} \sum_{l \neq k}^{N} \sum_{\alpha\beta} \frac{\partial M'_{k\alpha,l\beta}}{\partial B_{\mu ij}} C''_{l\beta,k\alpha} \ , \tag{A.17}$$

where we have introduced $C''_{i\alpha,j\beta}$ through

$$C''_{i\alpha,j\beta} = C'_{i\alpha,j\beta} - C'_{j\alpha,j\beta} \ . \tag{A.18}$$

Then we calculate $\frac{\partial M'_{k\alpha,l\beta}}{\partial B_{\mu ij}}$ explicitly, which yields

$$T_{\mu ij} = \sum_{\alpha\beta} \frac{(x_{i\rho} - x_{j\rho})}{\{(x_i - x_j)^2 + (\epsilon\ell)^2\}^2} \{(\tilde{\Gamma}_\sigma \tilde{\Gamma}^\dagger_\rho \tilde{\Gamma}_\mu)_{\alpha\beta} - (\tilde{\Gamma}_\mu \tilde{\Gamma}^\dagger_\rho \tilde{\Gamma}_\sigma)_{\alpha\beta}\} b_{\sigma ji} C'''_{i\beta,j\alpha} \tag{A.19}$$

for $i \neq j$ and

$$\begin{aligned} T_{\mu ii} \ = \ & \sum_{k \neq i}^{N} \sum_{\alpha\beta} \left[\frac{\delta_{\mu\rho}}{\{(x_i - x_k)^2 + (\epsilon\ell)^2\}^2} - \frac{4(x_{i\mu} - x_{k\mu})(x_{i\rho} - x_{k\rho})}{\{(x_i - x_k)^2 + (\epsilon\ell)^2\}^3} \right] \\ & (\tilde{\Gamma}_\sigma \tilde{\Gamma}^\dagger_\rho \tilde{\Gamma}_\tau)_{\alpha\beta} (b_{\sigma ki} b_{\tau ik} - b_{\sigma ik} b_{\tau ki}) C'''_{i\beta,k\alpha} \ , \end{aligned} \tag{A.20}$$

where we defined $C'''_{i\alpha,j\beta}$ through

$$\begin{aligned} C'''_{i\alpha,j\beta} \ &= \ C''_{i\alpha,j\beta} + C''_{j\alpha,i\beta} \\ &= \ C'_{i\alpha,j\beta} - C'_{j\alpha,j\beta} - C'_{i\alpha,i\beta} + C'_{j\alpha,i\beta} \ . \end{aligned} \tag{A.21}$$

Let us comment on the required computational effort of our algorithm. The dominant part comes from calculating the inverse in (A.15), which requires $O(n^3)$ arithmetic operations, where n is the size of the matrix to be inverted. In the present case n is of O(N). In order to keep the acceptance rate at the Metropolis accept/reject procedure reasonably high, one has to decrease the step size $\Delta\tau$ as one goes to larger N. We have seen from simulations that the step size should be taken to be $\Delta\tau \sim \frac{1}{\sqrt{N}}$, which is consistent with a general formula $\Delta\tau \sim V^{-1/4}$ in Ref. [34], where the system size V should be replaced by O(N^2) in our case. Accordingly, the number of steps for one trajectory increases as $\nu \sim \sqrt{N}$. Therefore, the required computational effort is estimated to be $O(N^{7/2})$.

In fact, one can reduce the computational effort by omitting the Metropolis accept/reject procedure, since in that case one can keep the step size $\Delta\tau$ fixed to a small constant for all N. The required computational effort becomes $O(N^3)$. The price one has to pay is that the algorithm then suffers from a systematic error due to the small violation of the Hamiltonian conservation. The systematic error can be estimated to be O($(\Delta\tau)^2$), see Appendix B.

Appendix B: Optimization of the algorithm

In this appendix, we first discuss the optimization of the parameters in the algorithm with the Metropolis accept/reject procedure. We then move on to the case when the Metropolis accept/reject procedure is omitted. The algorithm and the parameters used for each run is also described.

To start with, one can actually generalize the algorithm described in Appendix A by taking the step size $\Delta\tau_x$ for the diagonal elements to be different[8] from the step size $\Delta\tau$ for the off-diagonal elements of $B_{\mu ij}$ and $X_{\mu ij}$. We have fixed the ratio $\Delta\tau_x/\Delta\tau$ to be the ratio of the mean magnitudes of $x_{i\mu}$ and $b_{\mu ij}$, which we found from simulations to be approximately 1 for $D = 6$ and $1/2$ for $D = 10$, respectively.

We still have two parameters in the algorithm, i.e., $\Delta\tau$ and ν (the number of molecular dynamics steps for each trajectory), which can be optimized in a standard way [35, 36]. The key point of the optimization is that the autocorrelation time (in units of accepted trajectory) depends only on $\nu\,\Delta\tau = \tau$, but not on $\Delta\tau$ and ν separately. This allows us to perform the optimization in two steps. First, one fixes $\nu\,\Delta\tau = \tau$ and optimize $\Delta\tau$ so that the effective speed of motion in the configuration space, given by acceptance rate times $\Delta\tau$, is maximized. Second, using the optimized $\Delta\tau$ for each τ, one minimizes a typical autocorrelation time in units of molecular dynamics step with respect to τ.

In Fig. 5, we show the acceptance rate times $\Delta\tau$ as a function of $\Delta\tau$ for $D = 6$, $N = 16$ with fixed $\tau = 1.5$. We find that the optimal $\Delta\tau$ is 0.0375. For $D = 6, N = 32$ with fixed $\tau = 1.5$, we find that the optimal $\Delta\tau$ is 0.02142, which is smaller than for $N = 16$ as expected. For both cases, the acceptance rate at the optimal $\Delta\tau$ is found to be $50 \sim 60\%$.

Using the optimal $\Delta\tau$ obtained in the above way for each τ, we minimize a typical autocorrelation time (in units of molecular dynamics step) with respect to τ. Here, we measure the autocorrelation time of the extent R of the x_i-distribution defined in (4.2) and plot it as a function of τ. Fig. 6 shows the result for $D = 6$ with $N = 16$. We see that it has a minimum around $\tau \sim 1.5$. Similar experiments for $N = 32$ showed that the optimal τ is almost independent of N.

[8] This is not the case for the full model [18], where $\Delta\tau$ should be taken universally for each element of $A_{\mu ij}$ in order to respect the SU(N) invariance. In the present case, since the SU(N) "gauge" invariance is fixed by the "gauge-fixing" (3.4), we only have to respect the invariance under permutation of the SU(N) indices.

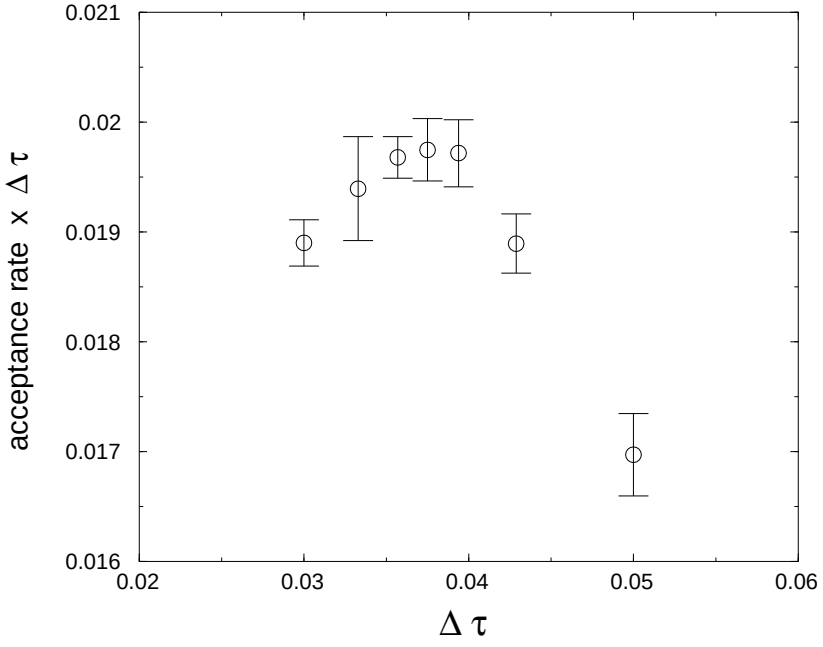

Figure 5: The acceptance rate times $\Delta\tau$ is plotted against $\Delta\tau$ for $D = 6, N = 16$ with fixed $\tau = 1.5$.

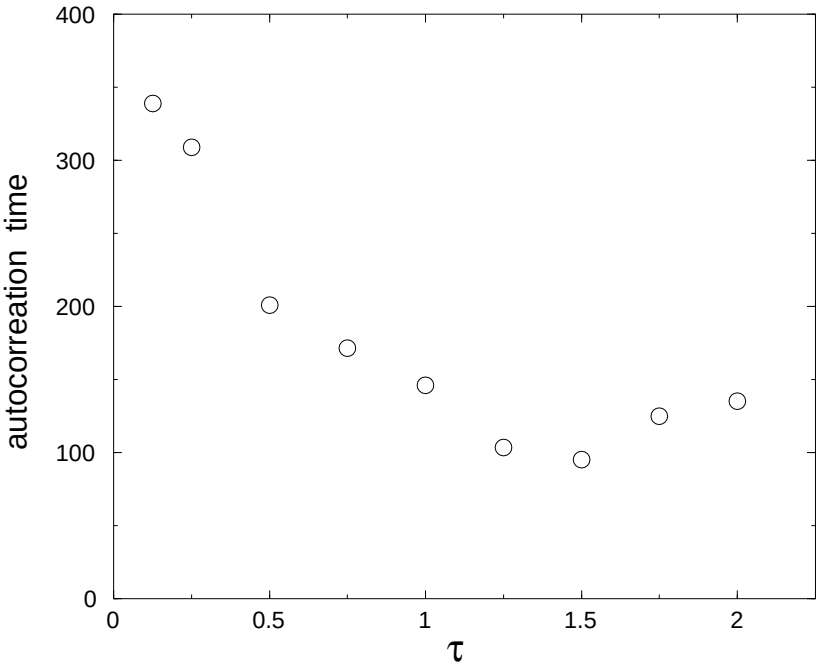

Figure 6: The autocorrelation time (in units of molecular dynamics step) of the extent R of the x_i-distribution is plotted against τ for $D = 6, N = 16$. $\Delta\tau$ is chosen for each τ so that the acceptance rate times $\Delta\tau$ is maximized.

When we omit the Metropolis accept/reject procedure, the algorithm suffers from a systematic error, as is explained in Appendix A. Here we fix $\nu\,\Delta\tau$ to the optimal τ obtained for the case with the Metropolis accept/reject procedure and study the $\Delta\tau$ dependence of the systematic error. As a quantity which shows a large systematic error, we take $\langle\lambda_1\rangle$, the expectation value of the largest eigenvalue of the moment of inertia tensor defined by (4.1). In Fig. 7, we plot the result against $(\Delta\tau)^2$ for $D = 6, N = 16$ with $\tau = 1.5$. The systematic error is seen to vanish as $\mathrm{O}((\Delta\tau)^2)$, which can be also understood theoretically by using the analysis described in Ref. [36].

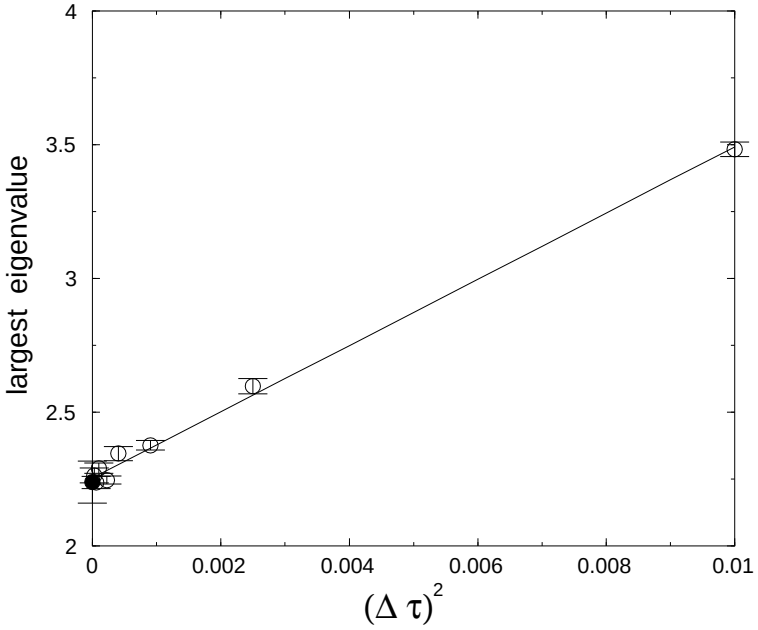

Figure 7: The expectation value of the largest eigenvalue of the moment of inertia tensor is measured by simulations *without* Metropolis accept/reject procedure. The result is plotted against $(\Delta\tau)^2$ for $D = 6, N = 16$ with fixed $\tau = 1.5$. The filled circle at $\Delta\tau = 0$ represents the result obtained by a simulation *with* Metropolis accept/reject procedure. The straight line is a fit to the predicted $(\Delta\tau)^2$ behavior of the systematic error.

Finally, let us comment on the algorithms and the parameters we used in our simulations at large N. The runs for $D = 6$ with $N = 192, 256$ were made by the algorithm including the Metropolis accept/reject procedure. The parameters are $\Delta\tau = 0.0048, \nu = 60$ for $N = 192$, and $\Delta\tau = 0.004, \nu = 50$ for $N = 256$. The numbers of configurations used for the measurements are 560 and 1732 for $N = 192$ and $N = 256$, respectively. (The optimization described in this Appendix was not completed when we started these runs. Accordingly, we needed significantly larger numbers of configurations compared to the cases below.) For the

other cases, we omitted the Metropolis accept/reject procedure in order to obtain a sufficient statistics. The parameters are $\Delta\tau = 0.0075, \nu = 200$ for $D = 10$ with $N = 192, 256, 384, 512$, and $\Delta\tau = 0.005, \nu = 300$ for $D = 6$ with $N = 512, 768$. The numbers of configurations used for the measurements are 88, 40, 84, 44 for $D = 10$ with $N = 192, 256, 384, 512$, and 64, 50 for $D = 6$ with $N = 512, 768$, respectively.

References

[1] T. Banks, W. Fischler, S.H. Shenker and L. Susskind, Phys. Rev. **D55** (1997) 5112.

[2] N. Ishibashi, H. Kawai, Y. Kitazawa and A. Tsuchiya, Nucl. Phys. **B498** (1997) 467.

[3] R. Dijkgraaf, E. Verlinde and H. Verlinde, Nucl. Phys. **B500** (1997) 43; V. Periwal, Phys. Rev. **D55** (1997) 1711; T. Yoneya, Prog. Theor. Phys. **97** (1997) 949; J. Polchinski, Prog. Theor. Phys. Suppl. **134** (1999) 158; H. Sugawara, hep-th/9708029; H. Itoyama and A. Tokura, Prog. Theor. Phys. **99** (1998) 129, Phys. Rev. **D58** (1998) 026002; K. Ezawa, Y. Matsuo and K. Murakami, Phys. Lett. **B439** (1998) 29.

[4] N. Kim and S.J. Rey, Nucl. Phys. **B504** (1997) 189; T. Banks and L. Motl, J. High Energy Phys. **12** (1997) 004; D.A. Lowe, Phys. Lett. **B403** (1997) 243; S.J. Rey, Nucl. Phys. **B502** (1997) 170; P. Horava, Nucl. Phys. **B505** (1997) 84; M. Krogh, Nucl. Phys. **B541** (1999) 87, 98.

[5] A. Fayyazuddin, Y. Makeenko, P. Olesen, D.J. Smith and K. Zarembo, Nucl. Phys. **B499** (1997) 159; C.F. Kristjansen and P. Olesen, Phys. Lett. **B405** (1997) 45; J. Ambjørn and L. Chekhov, J. High Energy Phys. **12** (1998) 007; S. Hirano and M. Kato, Prog. Theor. Phys. **98** (1997) 1371; I. Oda, Phys. Lett. **B427** (1998) 267; N. Kitsunezaki and J. Nishimura, Nucl. Phys. **B526** (1998) 351; T. Tada and A. Tsuchiya, hep-th/9903037.

[6] K.G. Wilson, Phys. Rev. **D10** (1974) 2445.

[7] H. Aoki, S. Iso, H. Kawai, Y. Kitazawa, A. Tsuchiya and T. Tada, Prog. Theor. Phys. Suppl. **134** (1999) 47.

[8] T. Eguchi and H. Kawai, Phys. Rev. Lett. **48** (1982) 1063.

[9] R.A. Janik and J. Wosiek, hep-th/0003121.

[10] J. Nishimura, Mod. Phys. Lett. **A11** (1996) 3049.

[11] T. Nakajima and J. Nishimura, Nucl. Phys. **B528** (1998) 355.

[12] W. Krauth, H. Nicolai and M. Staudacher, Phys. Lett. **B431** (1998) 31.

[13] W. Krauth and M. Staudacher, Phys. Lett. **B435** (1998) 350.

[14] T. Hotta, J. Nishimura and A. Tsuchiya, Nucl. Phys. **B545** (1999) 543.

[15] W. Krauth and M. Staudacher, Phys. Lett. **B453** (1999) 253.

[16] S. Oda and T. Yukawa, Prog. Theor. Phys. **102** (1999) 215.

[17] W. Krauth, J. Plefka and M. Staudacher, Class. Quant. Grav. **17** (2000) 1171.

[18] J. Ambjørn, K.N. Anagnostopoulos, W. Bietenholz, T. Hotta and J. Nishimura, `hep-th/0003208`.

[19] W. Krauth and M. Staudacher, `hep-th/0004076`.

[20] J. Ambjørn, A. Irbäck, J. Jurkiewicz and B. Petersson, Nucl. Phys. **B393** (1993) 571.
J. Ambjørn, J. Jurkiewicz, S. Varsted, A. Irbäck and B. Petersson, Phys. Lett. **B275** (1992) 295.

[21] M. Bowick, P. Coddington, L. Han, G. Harris and E. Marinari, Nucl. Phys. **B394** (1993) 791.
K. Anagnostopoulos, M. Bowick, P. Coddington, M. Falcioni, L. Han, G. Harris and E. Marinari, Phys. Lett. **B317** (1993) 102.

[22] J. Ambjørn and S. Varsted, Phys. Lett. **B257** (1991) 305.

[23] H. Aoki, S. Iso, H. Kawai, Y. Kitazawa and T. Tada, Prog. Theor. Phys. **99** (1998) 713.

[24] J. Ambjørn, M. Flensburg and C. Peterson, Phys. Lett. **B159** (1985) 335; Nucl. Phys. **B275** (1986) 375.

[25] W. Bietenholz, A. Pochinsky and U.-J. Wiese, Phys. Rev. Lett. **75** (1995) 4524.
S. Chandrasekharan and U.-J. Wiese, Phys. Rev. Lett. **83** (1999) 3116.

[26] S. Duane, A.D. Kennedy, B.J. Pendleton and D. Roweth, Phys. Lett. **B195** (1987) 216.

[27] P.B. Wiegmann, Nucl. Phys. **B323** (1989) 330.

[28] A.M. Polyakov, Nucl. Phys. **B268** (1986) 406.

[29] J. Ambjørn, B. Durhuus, J. Fröhlich and T. Jonsson, Nucl. Phys. **B290** (1987) 480.
J. Ambjørn, B. Durhuus and T. Jonsson, Phys. Rev. Lett. **58** (1987) 2619.

[30] J. Nishimura and G. Vernizzi, J. High Energy Phys. **04** (2000) 015.

[31] T. Suyama and A. Tsuchiya, Prog. Theor. Phys. **99** (1998) 321.

[32] D. Weingarten, Nucl. Phys. B (Proc. Suppl.) **9** (1989) 447.

[33] D.J.E. Callaway and A. Rahman, Phys. Rev. Lett. **49** (1982) 613.
J. Polonyi and H.W. Wyld, Phys. Rev. Lett. **51** (1983) 2257.

[34] S. Gupta, A. Irbäck, F. Karsch and B. Petersson, Phys. Lett. **B242** (1990) 437.

[35] R. Gupta, G.W. Kilcup and S.R. Sharpe, Phys. Rev. **D38** (1988) 1278.

[36] S. Gottlieb, W. Liu, D. Toussaint, R.L. Renken and R.L. Sugar, Phys. Rev. **D35** (1987) 2531.